Taylor & Francis
Taylor & Francis Group

ORIGINAL RESEARCH

Alternol triggers immunogenic cell death *via* reactive oxygen species generation

Changlin Li [ID][a,b], Ying Zhang[a], Siyuan Yan[a], Guoan Zhang[c], Wei Wei[d], Zhi Qi[e], and Benyi Li [ID][b]

[a]Institute of Precision Medicine, Jining Medical University, Jining China; [b]Department of Urology, The University of Kansas Medical Center, Kansas City, KS USA; [c]Institute of Cancer Pathology Research, Jining Medical University, Jining, China; [d]Center for Experimental Medicine, School of Public Health, Jining Medical University, Jining, China; [e]Department of Histology and Embryology, School of Medicine, Nankai University, Tianjin, China

ABSTRACT

Alternol is a naturally occurring compound that exerts antitumor activity in several cancers. However, whether Alternol induces antitumor immune response remains unknown. In this study, we investigated whether Alternol induced immunogenic cell death (ICD) in prostate cancer cells. Alternol triggered ICD in prostate cancer cells, as evidenced by the release of damage-associated molecular patterns (DAMPs) (i.e., calreticulin, CALR; high mobility group protein B1, HMGB1; and adenosine triphosphate, ATP) and pro-inflammatory cytokine (i.e., interleukin [IL]-1α, IL-1β, IL-6, and IL-8) expression. Alternol facilitated tumor-associated antigen uptake and cross-presentation, CD8 + T-cell priming, and T-cell infiltration in tumor-draining lymph nodes (LNs) and tumors. The presence of Alternol fostered antitumor immune response *in vivo*, resulting in delayed tumor growth and prolonged survival. Moreover, inhibition of reactive oxygen species (ROS) generation blocked Alternol-induced upregulation of pre-inflammation cytokines, endoplasmic reticulum (ER) stress, and consequent antitumor immune response. Overall, our data indicate that Alternol triggers ICD in prostate cancer cells, which is mediated by ROS generation.

Introduction

Prostate cancer (PCa) is the most frequently diagnosed cancer and the second-leading cause of cancer mortality in men in developed countries.[1] Although patients with PCa initially benefit from treatments (e.g., androgen deprivation therapy, androgen-receptor-signaling inhibitors, and chemotherapeutic agents), the prognosis for these patients remains poor due to drug resistance.[2,3] Cancer immunotherapy is considered the revolutionary therapeutic strategy for cancer, which induces long-lasting anti-tumor responses with few toxicity. Over the last decade, cancer immunotherapies, such as immune-checkpoint inhibitors (ICIs), adoptive T-cell therapy, and chimeric antigen receptor T-cells (CART), have succeeded in preclinical studies and cancer clinical therapies for several cancers including melanoma,[4–6] lung cancer,[7] breast cancer,[8] and B-cell lymphoblastic leukemia.[9] However, most of these immunotherapeutic strategies have only shown limited benefit for patients with PCa due to resistance and immunosuppression.[10,11] Therefore, novel interventions triggering antitumor immune response are required for the improved treatment of PCa.

Cell death elicited by specific stimuli (such as chemotherapy and radiotherapy) triggers a potent antitumor immunity response (known as immunogenic cell death, or ICD).[12] The released DAMPs (damage-associated molecular patterns) and pro-inflammatory cytokines are associated with the apoptotic cells that undergo ICD, and this facilitates tumor-associated antigen uptake and cross-presentation to T cells, and eventually activates cytotoxic T-lymphocyte activity against tumors.[13,14] Recent studies have revealed that certain anticancer drugs, including anthracycline,[15,16] bortezomib,[17] oxaliplatin,[18] crizotinib,[19] dactinomycin,[20] and mitoxantrone,[21] foster ICD and induce immune response against tumor growth. Interventions targeting ICD not only directly induce cancer cell death but also trigger antitumor immune responses, and these are promising for the formulation of anti-tumor strategies.[22,23]

Alternol is a novel, naturally occurring compound isolated and purified from microbial fermentation products that are obtained from the bark of the yew tree in Kunming, China. Previous studies have demonstrated that Alternol exhibits antitumor activity against several cancers via induction of cell death.[24–28] However, whether Alternol-induced cell death triggers immune response against prostate cancer remains unknown. In this study, we investigated whether Alternol triggered ICD in prostate cancer cells, determining by the release of DAMPs, increased numbers of antigen presenting cells (APC) and T-cell activation.

Materials and methods

Cell lines, reagents, antibodies

Human prostate cancer cells (i.e., LNCaP, 22RV1, PC-3), human embryonic kidney 293 T cells, murine prostate cancer cells RM-1, and murine melanoma cells B16-F0 were obtained from ATCC (Manassas, VA). LNCaP, 22RV1, PC-3, and RM-1 cells were cultured in RPMI 1640 medium, supplemented with 10% fetal bovine serum (FBS) (Gibco) plus 100 U/ml

penicillin/streptomycin and 2 mmol/L L-glutamine (Gibco). B16-F0 and 293 T cells were cultured using Dulbecco's Modified Eagle's Medium medium supplemented with 10% FBS plus 100 U/ml of penicillin/streptomycin and 2 mmol/L L-glutamine. Antibodies were listed as Table S1. Dimethyl sulfoxide (DMSO), ovalbumin (257–264) chicken, and propidium iodide (PI) were obtained from Sigma (St. Louis, MO, USA). Alternol was a kind gift from Strand Biotech Co (Shantou, China). Carboxyfluorescein succinimidyl ester (CFSE), mitoxantrone (MTX), and N-Acetylcysteine (NAC) were obtained from MCE (New Jersey, NJ, USA). CellTracker™ Deep Red and CMFDA were ordered from ThermoFisher Scientific (Shanghai, China). Febuxostat (FBX) was obtained from CSNpharm (Shanghai, China).

Measurement of extracellular ATP and HMGB1 levels

After conduction of the indicated treatment, cell culture media were collected and subjected to ATP (adenosine triphosphate) and HMGB1 (high mobility group protein B1) protein assays. ATP levels were measured using an enhanced ATP Assay Kit (Beyotime Institute of Biotechnology, Jiangsu, China). HMGB1 protein levels were determined using an enzyme-linked immunosorbent assay (IBL International, Hamburg, Germany). Absorbance was measured using the Cytation-i5 Cell Imaging Reader (Biotek, USA).

Real time PCR

Real-time PCR was performed as in our previous studies.[29] Briefly, total RNA was extracted from cells using the Trizol reagent (Invitrogen) following the manufacturer's instructions. 1 µg RNA was subjected to reverse transcription (RT) using a 5× All-In-One RT MasterMix reverse Transcription Kit (ABM Company, Canada). Real-time PCR analysis was performed using a SYBR Green qPCR kit (ABM Company, Canada). 18S rRNA was used as an endogenous control. Real-time PCR was performed with LightCycler® 480 (ROCHE Diagnostic Spa). The relative expression level, expressing as a "change fold," was calculated with the $2^{[-\Delta\Delta Ct]}$ method. The primer sequences were described as Table S2.

Flow cytometry

CALR (calreticulin) exposure was determined as described in previous studies.[30,31] Briefly, 5×10^5 cells per treatment were subjected to staining with an anti-CALR antibody (1:100) for 40 min. After washing three times with phosphate buffered saline (PBS), cells were incubated with PI (1 µg/ml) for 10 min, and were then incubated with fluorescein isothiocyanate (FITC)-labeled anti-rabbit IgG (1:200) for 30 min. To exclude dead cells, CALR-positive cells were gated on PI-negative cells.[32]

To determine the surface markers of dendritic cells (DCs), spleen tissues of male C57BL/6 mice were dissociated into single cells by incubating with collagenase IV. Red blood cells were removed using an ammonium chloride-potassium (ACK) lysis buffer (Gibco, catalog# A1049201). Cells were co-incubated with four marker antibodies for 30 min, by using one antibody against general surface markers of DCs (i.e., anti-CD69, CD80, and CD86 antibodies) and three other antibodies, namely, phycoerythrin [PE]/sulfo-Cyanine7 [Cy7]-conjugated CD11 c, FITC-conjugated CD8a, and PE/PC5.5-conjugated B220. PE-isotype-matched IgG antibodies were used as negative control. In the flow cytometer, the cells were gated on CD8a+ DCs ($CD8a^+/B220^-/CD11c^+$) cells.

For myeloid-derived suppressor cells (MDSCs) and regulatory T cells (T_{reg}) analysis, mouse spleen tissues were subjected to enzymatic digestion to obtain single cells. After removal of red blood cells using an ACK lysis buffer, cells were incubated with the indicated antibodies. MDSCs numbers were determined by performing co-staining using CD11b, Ly6C, and Ly6G antibodies. Cells were gated on CD11b-positive cells. T_{reg} counts were obtained by performing staining for CD25, CD4, and FoxP3. Cells were first incubated with anti-CD25, CD4 antibodies for 30 min followed by fixation with 0.5% paraformaldehyde. Fixated cells were permeabilized with 0.1% Triton X-100 (which included mouse FcR) for 10 min and then incubated with FoxP3 antibody for 30 min. Cells were gated on CD25-positive cells.

Flow cytometry was performed using the CytoFLEX (Beckman, Germany). Mean fluorescence intensity (MFI) and cellular population were analyzed by CytExpert soft (V.2.3.0.84).

Phagocytosis assay

Human DCs induction and phagocytosis assays were performed as previously described.[30,31] Briefly, human peripheral blood mononuclear cells (PBMCs) were isolated from healthy donors by using a Lymphoprep kit (STEMCELL, catalog# 07801). Monocytes were enriched via immunomagnetic cell separation using an anti-CD14 MicroBeads (Miltenyi Biotec, catalog #130–050–201). To obtain the immature DCs, enriched monocytes were cultured for 6 days, supplemented with granulocyte macrophage-colony-stimulating factor (GM-CSF) (100 ng/ml, Peprotech) and IL-4 (100 ng/ml, Peprotech). Prostate cancer cells were subjected to treatment with DMSO, MTX (1 µM), and Alternol (10 µM) for 16 h, followed by incubation with 0.5 µM CFSE for 15 min. Immature DCs were labeled with CellTracker Deep. CellTracker Deep-labeled DCs and CFSE-labeled tumor cells were co-cultured for 4 h. Percentage of phagocytosis was determined by flow cytometry, as previously described.[31]

RM-1-Oval (chicken ovalbumin) cells constructs

The lentivirus vectors pLVX-puro-cOVA was a gift from Maria Castro (Addgene, catalog # 135073) expressing a model antigen peptide SIINFEKL (Ser-Ile-Ile-Asn-Phe-Glu-Lys-Leu). Lentivirus were packaged as described before.[29] Briefly, psPAX2/pMD2.G (Addgene, catalog # 12259, 12260) and pLVX-puro-cOVA vector were co-transfected into 293 T cells. These RM-1 cells were subjected to infection with supernatants containing the lentivirus and were then selected using puromycin (Gibco, catalog #A1113802, 1 µg/ml).

In vivo studies

Six-week-old male C57BL/6 mice and severe combined immunodeficiency (SCID) mice were purchased from Vital River

Laboratory Animal Technology (Beijing, China). OT-I CD8 + T cell receptor (TCR)- Tγ mice were obtained from Jackson Laboratory. Mice were housed in a specific pathogen free (SPF) facility in our laboratory animal center (Jining Medical University). All procedures were performed in accordance with the protocol approved by the Institutional Animal Care and Use Committee of Jining Medical University.

Mouse xenograft models and Alternol administration

Mouse xenografts were generated as described in our previous study.[25] Briefly, RM-1 cells (1×10^6) were injected subcutaneously into the flanks of 6-week-old male SCID and C57BL/6 mice. At 7 days after injection, mice were randomly divided into two groups ($n = 8$) and treated with solvent and Alternol, respectively. Alternol was administered intraperitoneally at a dose of 20 mg/kg every 3 days until the mice were sacrificed. Mice were sacrificed using CO_2 inhalation, when maximum tumor diameter was close to 1.5 cm.

Animal vaccination

To induce ICD *in vivo*, tumor cells (1×10^6) were injected subcutaneously into the left flanks of six-week-old male C57BL/6 mice at day −20. Ten days after tumor cells inoculation, Alternol and MTX were administered intraperitoneally at a dose of 20 mg/kg and 3 mg/kg every day for 5 days, respectively. Tumors were surgically removed from the left flanks of mice under isoflurane anesthesia after inoculation for 20 days. Meanwhile, RM-1 cells (1×10^6) were injected subcutaneously into the right flank of mice. Tumor growth and survival studies were conducted.[33]

Mice vaccination *in vitro* was performed as described in previous studies.[31] Briefly, 1×10^6 RM-1 or RM-1-Ova cells were subjected to treatment as indicated and then injected into the left flank of C57BL/6. Freeze-thawed DMSO-treated cells were used as control treatment. One week after vaccination, 1×10^6 RM-1 or RM-1-Ova cells were injected into the right flank of male C57BL/6 mice.

T-cell infiltration assessment

Tumor-draining LNs and tumors were obtained from mice and subjected to formalin-fixation, dehydration, and paraffin-embedding, as in our previous publication.[34] Following antigen retrieval with sodium citrate buffer (pH 6.0), 4 μm-thick paraffin-embedding tissue section slides were stained with FITC-CD3 + antibody, followed by Hoechst 33342 staining to visualize the nuclei. The microscopic images were acquired using a confocal microscope LSM 800 Zeiss (Carl Zeiss Micro-Imaging, Inc.).

Cross-presentation analysis

Cross-presentation analysis was performed as previously described.[33] Male C57BL/6 mice were vaccinated with Alternol-treated RM-1 cells, tumor-draining LN was dissociated and then splintered to a single-cell suspension at day 20 and 35 days after vaccination, respectively. Percentage of H-2K^b-Ova+ DCs among tumor-draining LN and tumor was determined by flow cytometry using PE/Cy7 anti-mouse CD11c, and PE anti-mouse H-2Kb. PE-conjugated mouse IgG was used as the isotype control for the anti-H-2kb-OVA antibody.

CD8 + T-cell priming assay

CD8 + T-cell priming was determined via assessment of the proliferation of OVA $^{257-264}$-specific T-cells (OT-I) and IFNγ production as previously described.[33] Mice were vaccinated with DMSO- and Alternol-treated RM-1-Ova cells at day 0. CD8+ OT-I T-cells were isolated and enriched from the spleen tissues of OT-I CD8 + T-cells receptor (TCR)-Tγ mice using the CD8a+ T-Cell Isolation Kit (Miltenyi Biotec, catalog# 130–104–075) according to the manufacturer's instructions. Ten days after vaccination, 2×10^6 CFSE-labeled CD8+ OT-I T cells were intravenously injected into mice. Proliferation of CSFE-labeled OT-I T-cells from tumor-draining LN cells was determined by flow cytometry at day 15 after vaccination.

Interferon (IFN)-γ expression of CD8 + T cells was measured as previously described.[35] Briefly, mice were vaccinated with DMSO- and Alternol-treated RM-1-Ova cells on day 0. Mice injected intraperitoneally 50 μg ovalbumin (257–264) peptide were used as a positive control. After 5 days of vaccination, LNs were extracted from mice and digested into single cells. CD8 + T cells were enriched via immunomagnetic cell separation microBeads CD8a+ T Cell Isolation Kit (Miltenyi Biotec, catalog# 130–104–075). After re-stimulated with ovalbumin (257–264) peptide (40 μg/ml) for 72 h, IFN-γ production in the culture medium was measured using a mouse IFNγ ELISA kit (BD Biosciences, catalog#555138). Absorbance was measured using the Cytation-i5 Cell Imaging Reader (Biotek, USA).

CD8 + T-cell depletion and adoptive CD8 + T-cell transfer assay

CD8 + T-cell depletion was performed as previously described.[35] Briefly, anti-CD8 antibodies (clone 53–6.7) were injected by i.p at days −9, −8, 0, and 7 at a dose of 10 mg/kg. Rat IgG2a, κ was used as an isotype control. An adoptive T-cell transfer assay was performed as previously described.[30] CD8 + T-cells were isolated from tumor-draining LNs and tumors of mice vaccinated with DMSO- and Alternol-treated RM-1 using the CD8a+ T cell isolation kit (Miltenyi Biotec, catalog# 130–104–075) and were then adoptively transferred intravenously into C57BL/6 J mice recipients at day −5. Parental RM-1 cells at a density of 5×10^5 cells per mouse were injected into the flank at day 0. Tumor growth and survival were assessed.

RNA-sequencing analysis

PC-3 cells were treated with 10 μM Alternol and DMSO for 16 h followed RNA-sequencing. Sequence was performed using BGISEQ-500 platform. After removing the low-quality and adaptor-polluted reads from the raw data, clean reads were used to map to reference transcripts using Bowtie2.[36] RSEM[37] and DEseq2[38] were used to calculate genes expression level and identify differentially expression genes (DEGs). DEGs were subjected to pathway classification and functional enrichment, using KEGG (Kyoto Encyclopedia of Genes and Genomes).

Statistical analysis

Data are presented as means ±s.e.m. from at least three independent experiments. One-way analysis of variance (ANOVA)

and Student's t-test were performed to determine the statistical significance of multiple groups and two groups, respectively. Differences in growth curves were measured using two-way ANOVA. Overall survival and tumor-free curves were determined by Log-rank (Mantel-Cox) test. All statistical analyses were performed using GraphPad Prism 8.0.2 software (GraphPad). Differences were considered statistically significant when p values were greater than 0.05.

Results

Alternol triggers the release of DAMPs and phagocytosis by DCs

To investigate the effect of Alternol treatment on ICD, we examined whether Alternol induced CALR exposure, and the release of HMGB1 and ATP, which are characteristic of ICD.[13,14] MTX, a *bona fide* strong ICD, was used as a positive control in this study. Prostate cancer cell lines PC-3, LNCaP, and 22RV1 were subjected to treatment with Alternol, MTX,

DMSO for 16 h. CALR exposure was determined by flow cytometry. CALR-positive cells were gated on PI-negative cells (Supplemental Figure S1a-d). Both Alternol and MTX treatments significantly increased CALR exposure on the cell surface of PC-3 (Figure 1a, d), LNCaP (Figure 1b, e), and 22RV1 (Figure 1c, f) compared with DMSO treatment. However, there was lower CALR exposure in MTX-treated PC-3, LNCaP, and 22RV1 cells compared with those treated with Alternol (Figure 1a-f). Similarly, Alternol and MTX treatment significantly elevated the levels of HMBG1 in PC-3, LNCaP, and 22RV1 cells compared with DMSO treatment (Figure 1g). Consistent with CALR exposure, Alternol treatment favored the release of ATP in PC-3, LNCaP, and 22RV1 cells compared with MTX and DMSO treatment (Figure 1h). Furthermore, we examined whether Alternol affected phagocytosis by DCs. Alternol-induced apoptosis in PC-3, LNCaP, and 22RV1 cells was associated with enhanced rate of phagocytosis by DCs compared with MTX and DMSO treatment (Figure 2a, b). These findings suggest that Alternol induces the release of DAMPs and phagocytosis by DCs *in vitro*.
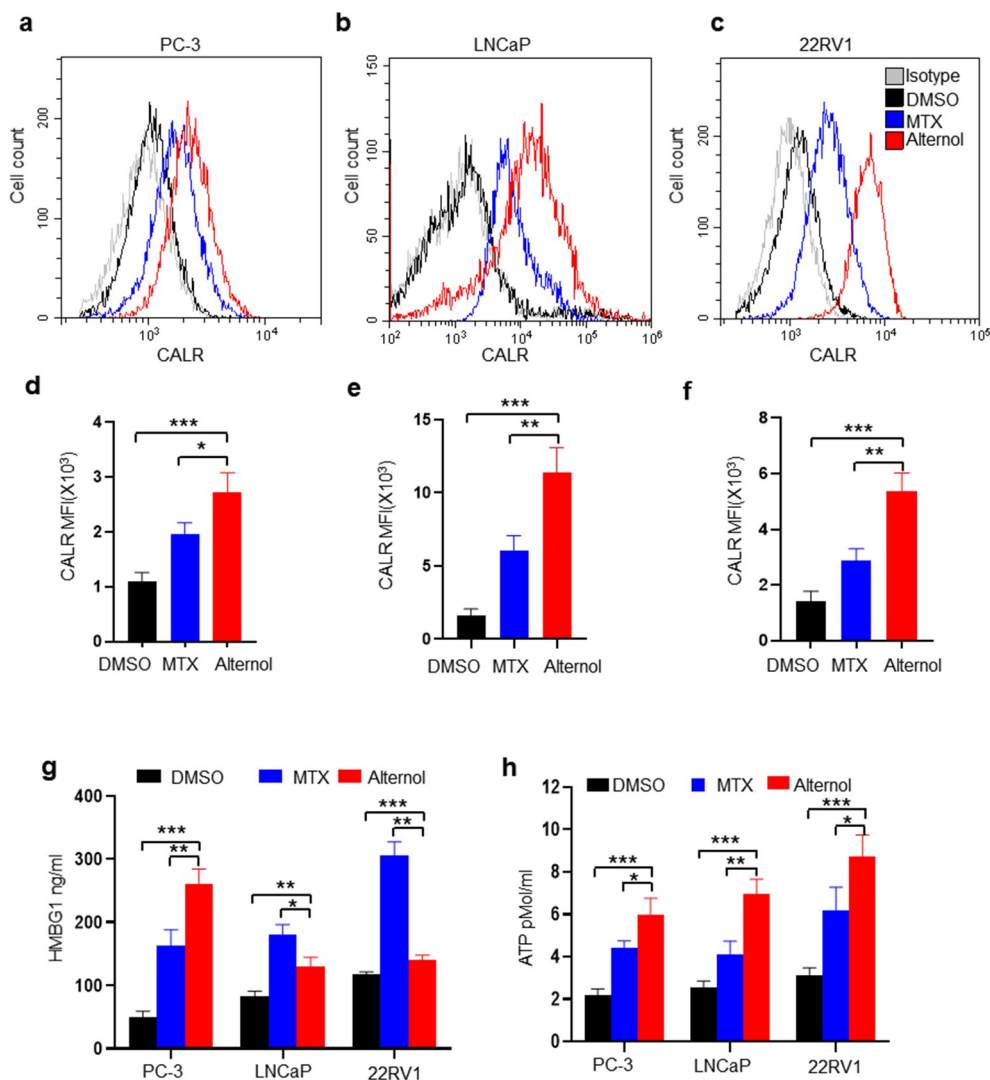
Figure 1. Alternol triggers release of DAMPs. PC-3, LNCaP and 22RV1 cells were treated with DMSO, MTX (1 μM), and Alternol (10 μM) for 16 h. (a-c) Representative flow cytometry plots. CALR translocation was measured by flow cytometry analyses. (d-f) Quantitative data for CALR translocation. (g) Release of HMBG1 in PC-3, LNCaP, and 22RV1 cells were determined by ELSA. (h) Release of ATP was measured by Luc-report analyses. Data from four independent experiments are presented as means ± s.e. m. (one-way ANOVA; * $p < .05$, ** $p < .01$, ***$p < .001$).
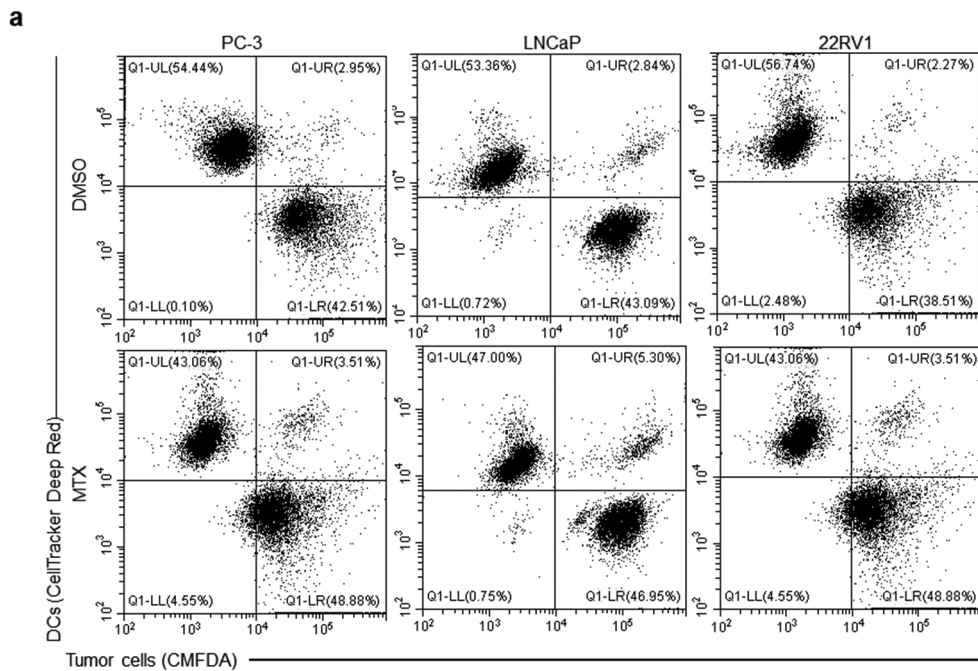
Figure 2. Aternonl treatment enhances phagocytosis by dendritic cells (DCs). (a-b) CellTracker Deep Red labeled DCs were incubated with CMFDA labeled LNCaP cells treated with DMSO, MTX (1 μM), and Alternol (10 μM) for 2 h. (a) Representative flow cytometry analyses of phagocytosis by DCs. (b) Quantification of four independent experiments. Error bars are s.e.m. (one-way ANOVA; * $p < .05$, ***$p < .001$).
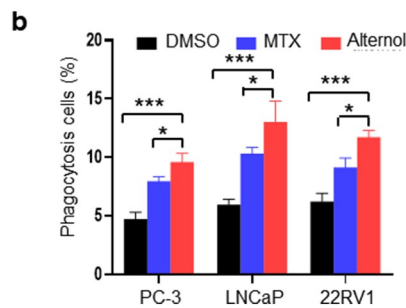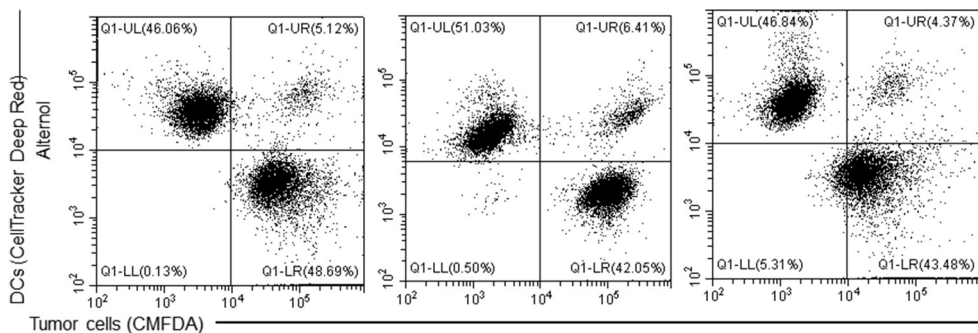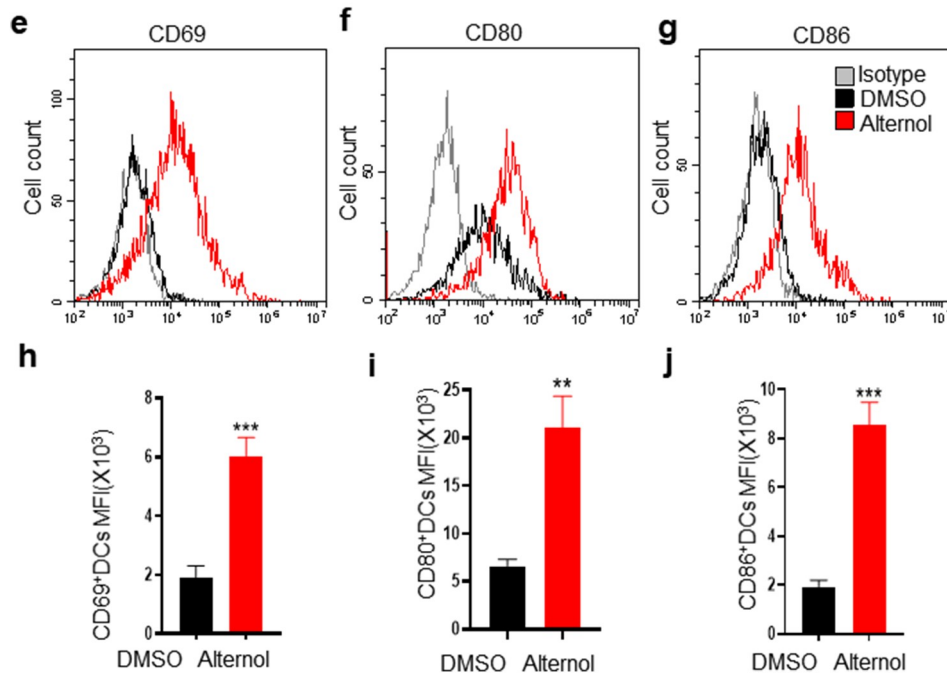

Figure 2. Continued.

Alternol triggers anti-tumor immune responses in vivo

A vaccination assay is the gold standard for the determination of immunogenic cell death *in vivo*.[13] To further evaluate the effect of Alternol on ICD, we subcutaneously injected RM-1 tumor cells (1×10^6) into the left flank of 6-week-old male C57BL/6 mice at day −20 days. To induce ICD *in vivo*, Alternol and MTX were administered intraperitoneally at a dose of 20 mg/kg and 3 mg/kg every day

for 5 days, respectively, beginning at day −10 after tumor cells inoculation. MTX was used as a positive control. Tumors were surgically removed from mice at 20 days after inoculation. Meanwhile, the mice were re-challenged with live parental RM-1 cells injected into the right flank of mice (Figure 3a). Mice vaccinated with Alternol-treated RM-1 presented with retarded tumor growth (Figure 3b), delayed tumor progression (Figure 3c), and prolonged
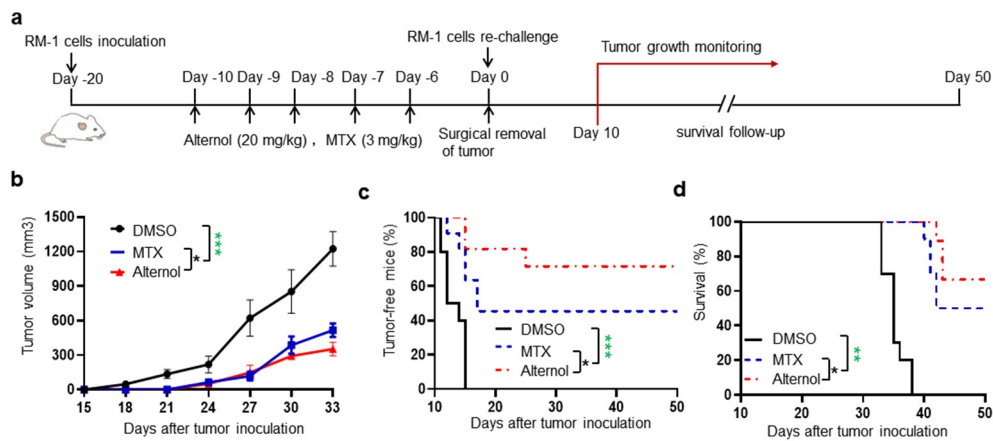
Figure 3. Alternol triggers antitumor immunity *in vivo*. (a-i) RM-1 cells (1 × 10⁶) were injected subcutaneously into the flanks of 6-week-old male C57BL/6 mice. Ten days after tumor cells inoculation, Alternol and MTX were administered intraperitoneally at 20 mg/kg and 3 mg/kg, respectively, every day for 5 days. Tumors were surgically removed from mice at day 20 after inoculation. One week after tumor removal, mice were re-challenged with RM-1 cells (a). Tumor volume (*n* = 10, per group) (b), tumor-free and survival (*n* = 10, per group) (c, d) were monitored as indicated days. (e-g) Splenocytes were isolated from mice injected with DMSO- and Alternol (10 μM)- treated RM-1 cells. Surface markers CD69 (e, h), CD80 (f, i) and cd86 (g, j) of DCs were analyzed by flow cytometry (*n* = 5 mice per group). (e-g) Representative flow cytometry plots. (h-i) Quantitative data for CD69, CD80, CD86 expression. Two-way ANOVA analysis was performed to determine the statistical significance of tumor growth (b). Differences between tumor-free progression and animal overall survival were determined by Log-rank (Mantel-Cox) test analysis (c, d). One-way ANOVA was performed to determine the statistical significance of the two groups (h-g). The asterisks indicate significant differences between the indicated groups (** *p* < .01, *** *p* < .001).

Figure 3. Continued.

mouse survival (Figure 3d), compared with those observed in the mice vaccinated with MTX-treated and control mice. These data indicate that Alternol triggers ICD in prostate cancer cells *in vivo*. Moreover, Alternol treatment exerted more potent anti-tumor activity compared with that of MTX treatment.

To validate whether Alternol-induced anti-tumor immune response was the only effective mechanism against a specific cancer type, we vaccinated mice with Alternol-induced RM-1 cells that underwent cell death and then the mice were re-challenged with RM-1 and B16 cells, respectively

(Supplemental Figure S2a). Vaccination performed using RM-1 cells that underwent cell death significantly delayed RM-1 re-challenge-associated tumor growth and tumor incidence, but not that of B16 cells re-challenge (Supplemental Figure S2b, c). These data indicate that Alternol-induced anti-tumor immune response was elicited against a specific cancer type.

DCs activation and T-cell infiltration are notable features of anti-tumor immune response.[39] As such, we examined whether DC activation and T-cell infiltration were involved in Alternol-induced anti-tumor activity. DC activation was determined by

flow cytometry. The cells were gated on CD8a+ DCs (CD8a+/B220−/CD11c+) cells (Supplemental Figure S3a-f). Mice vaccinated with Alternol-induced dying RM-1 cells that underwent cell death presented high expression levels of early activation marker CD69 and costimulatory molecule (CD80 and CD86) expression compared with that observed in control mice (Figure 3e-f, h-j). Similarly, Alternol significantly increased T-cell infiltration in tumor-draining LNs (Figure 4a, b) and in tumors (Figure 4c, d). This evidence suggests that DC activation and T-cell infiltration are associated with the occurrence of Alternol-induced ICD.

T_{reg} and MDSCs are well known for their roles in immunosuppressive role during tumor development.[40,41] Furthermore, we determined whether Alternol affected T_{reg} and MDSCs. C57BL/6 mice were vaccinated with Alternol- and DMSO-treated RM-1 cells. The percentage of T_{reg} and MDSCs in spleen tissues obtained from tumor-bearing mice was analyzed by flow cytometry. Monocytic MDSCs (M-MDSC, CD11b+Ly6C^{high}Ly6G−) and polymorphonuclear MDSCs (PMN-MDSCs, CD11b+Ly6C^{low} Ly6G+) were gated on CD11b+ (Supplemental Figure S4a-d).[42] T_{reg} cells were gated on CD25+ cells (Supplemental Figure S5a-d). There was no significant difference between estimates obtained from mice vaccinated

with Alternol and those obtained from mice vaccinated with DMSO-treated RM-1 cells in M-MDSCs and PMN-MDSCs (Supplemental Figure S6a, b). Interestingly, Alternol treatment significantly inhibited T_{reg} cells (CD4+CD25+FoxP3+ T_{reg}) (Supplemental Figure S6c, d). These findings indicate that Alternol may confer protection against tumor development in vivo, by shifting the tumor microenvironment toward an environment that leads to the generation of immune activation responses rather than immunosuppression.

To further verify the role of Alternol in the elicitation of an anti-tumor immune response, we generated SCID and C57BL/6 mice xenograft models with RM-1 cells and then subjected the models to treatment with Alternol and solvent (Figure 4e). Alternol treatment exerted more potent anti-tumor activity in C57BL/6 mice xenograft model compared with that observed in the SCID mice xenograft model (Figure 4f, g). These data suggest that Alternol treatment triggers the establishment of anti-tumor immunity in vivo.

Alternol activates cross-presentation and T cell priming

To investigate the effect of Alternol-induced apoptotic tumor cell exposure on antigen cross-presentation, C57BL/6 mice
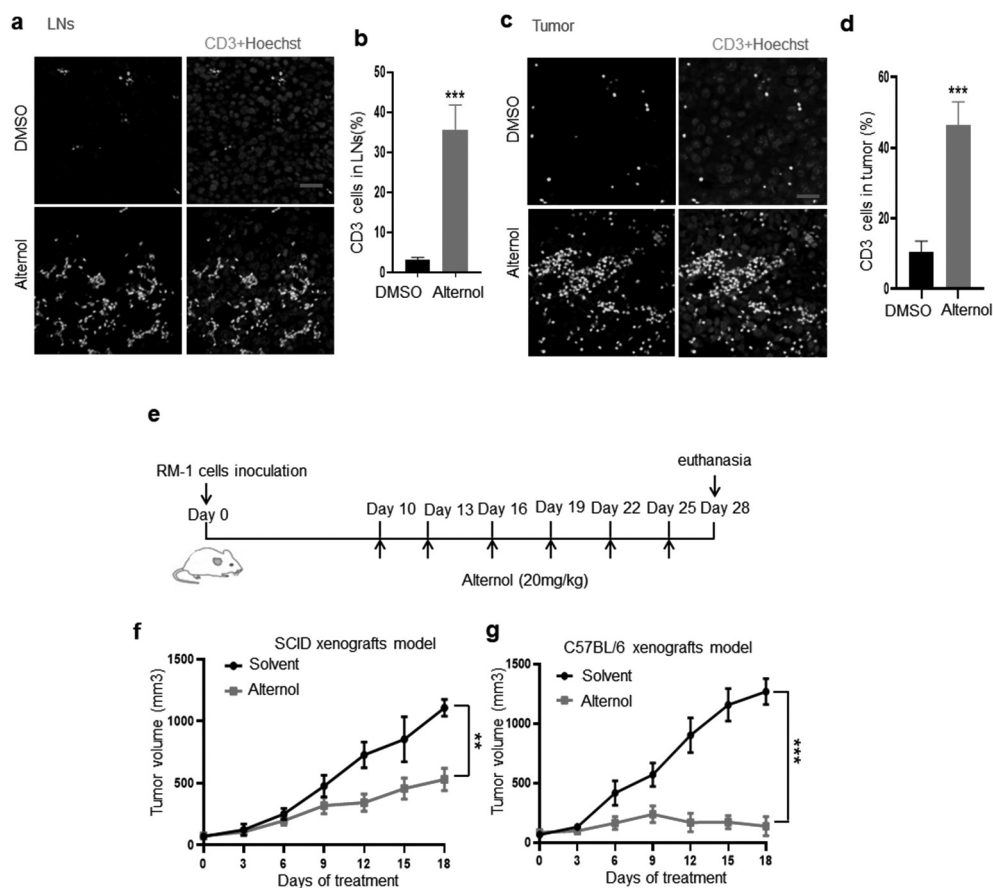
Figure 4. Alternol triggers T-cell infiltration. (a-d) Six-week-old male C57BL/6 mice were injected withRM-1 cells and administered intraperitoneally Alternol to induce ICD in vivo as shown in (Figure 3a). Tumor-draining LNs and tumors were removed from mice on day 33 after vaccination. T-cell infiltration in tumor-draining LNs (a, b) and tumors (c, d) were determined by CD3 staining. (a, c) Representative flow cytometry plots. Scale bars, 20 μm. (b, d) Quantitative data (n = 4 mice per group). (e) RM-1 cells (1 × 10^6) were injected subcutaneously into the flanks of 6-week-old male SCID and C57BL/6 mice (n = 8, per group). Alternol was administered intraperitoneally at 20 mg/kg every 3 days. DMSO (20%) in corn oil was as Solvent control. Tumor volume was monitored as indicated days (f, g). Statistical significance of the two groups was performed using student's t-test (b, d). Differences in tumor growth were determined using a two-way ANOVA analysis (f, j). The asterisks indicate significant differences between the indicated groups (** p < .01, *** p < .001).

were vaccinated with Alternol-induced dying RM-1 OVA cells that underwent cell death. The percentage of H-2K^b-OVA$^+$ (a complex of the OVA peptide [SIINFEKL] with H-2kb [MHC-I]), CD11c DCs of tumor–draining LNs were determined by performing flow cytometry using CD11c and an antibody that could recognize ovalbumin-derived peptide SIINFEKL bound to H-2Kb (Figure 5a, Supplemental Figure S7a-c). Alternol treatment resulted in cross-presentation of SIINFEKL on the surfaces of DCs obtained from tumor-draining LNs (Figure 5b, c).

To investigate the effect of Alternol on T-cell activation, IFNγ expression and T-cell proliferation were assayed *in vivo*, as indicated in Figure 5a. CFSE-labeled OT-I CD8 + T cells obtained from the spleen of OT-I mice were adoptively transferred into C57BL/6 mice vaccinated with Alternol-treated RM-Ova cells (Figure 6a). CD8 + T-cell proliferation was determined by the level of CFSE dilution, using flow cytometry (Supplemental Figure S8a-c). Alternol treatment significantly enhanced T-cell proliferation (Figure 6b, c). Alternol treatment significantly increased the levels of IFNγ production in CD8 + T-cells compared to that observed with DMSO treatment (Figure 6d).

To verify whether CD8 + T-cell activation was critical for Alternol-induced antitumor immunity, we blocked CD8$^+$ T cells with anti-CD8+ antibody *in vivo* (Figure 6e). T-cell blockade significantly inhibited Alternol-induced ICD *in vivo*, as indicated by the extents of tumor growth (Figure 6f), tumor incidence (Figure 6 g), and survival (Figure 6h). Subsequently, we isolated T cells from mice vaccinated with Alternol- and DMSO-treated RM-1 cells and then transferred adoptive T cells into naïve C57BL/6 mice. The naïve mice were challenged with RM-1 cells (Figure 6i). Compared with the control treatment, the transfer of T cells from mice vaccinated with Alternol-treated RM-1 cells seemed to confer protection against tumor growth (Figure 6j) and tumor incidence (Figure 6k), and prolonged survival (Figure 6l). Overall, these findings indicate that Alternol may activate cross-presentation and T-cell priming. Moreover, T-cell activity is necessary for Alternol-induced ICD.

### Alternol facilitates the release of pro-inflammatory cytokines

To further study the mechanism underlying Alternol-induced ICD, PC-3 cells were subjected to treatment with Alternol and DMSO for 16 h and then was performed global RNA sequencing to determine gene expression patterns. Based on the expression fold change and significance (|log2 (fold change) | >1, P < .05), 168 DEGs were identified in this study, including 101 up-regulated and 67 down-regulated genes. To identify the hub genes and associated pathway involved in alternol-induced ICD, DEGs were subjected to KEGG pathway analysis. The result showed that the hallmark pathway with the most considerable number of DEGs (CCL20, CXCL2, CXCL3, IL-8, IL1A, IL1B, IL2RB, IL6, IL7R, INHBE, and TNFSF10) was cytokine–cytokine receptor interaction, which is closely related to inflammation (Figure 7a). Enriched DEGs except for TNFSF10 were significantly upregulated in Alternol-treated PC-3 cells compared with that observed with DMSO treatment (Figure 7b). These results indicate inflammation is associated with the occurrence of Alternol-induced cell death.

### Reactive oxygen species (ROS) production is necessary for Alternol-induced ICD

Inflammatory responses are essential to ICD.[43] Our previous studies had shown that Alternol was appreciably efficient at inducing ROS production,[24] which triggers the release of
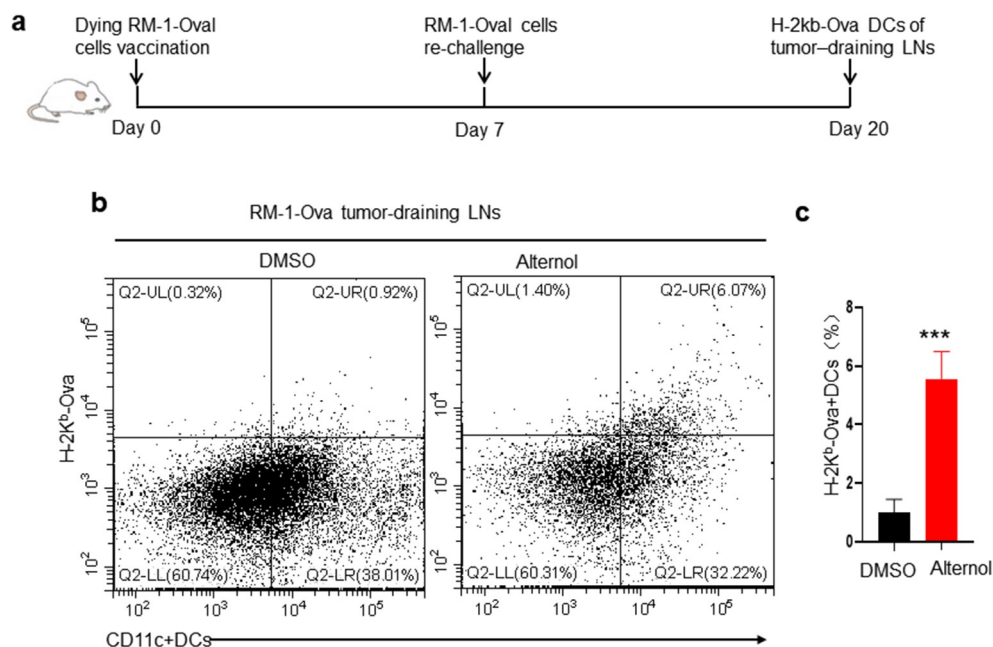
Figure 5. Alternol activates cross-presentation. (a) Experimental scheme for cross-presentation assay *in vivo*. RM-1-Ova cells were treated with DMSO and Alternol (10 μM) for 16 h. C57BL/6 mice were vaccinated with DMSO- and Alternol-treated RM-1-Ova cells. After 1 week, mice were re-challenged with RM-1-Ova cells. Tumor-draining LNs were dissociated from mice at 20 days. H-2Kb-OVA expression of CD8+ DCs was determined by flow cytometry. (b) Representative flow cytometry plots. (c) Quantitative data for the percentage of H-2Kb-OVA DCs (n = 5 mice per group). Error bars are means ±s.e.m. (Student's t-test, ***p < .001 versus DMSO treatment).
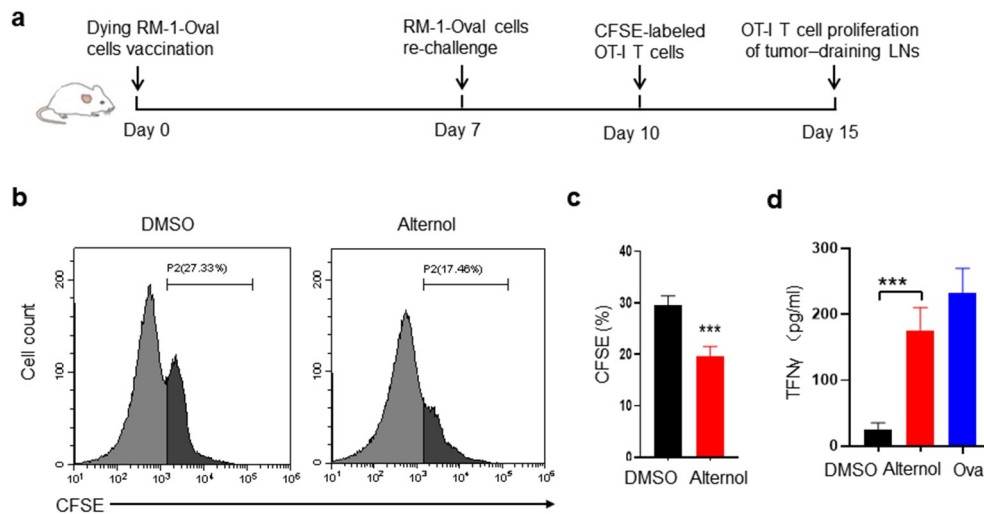
Figure 6. Alternol-induced ICD is mediated by CD8 + T cells. (a) Experimental scheme for CD8 + T-cell priming. Alt-induced apoptotic RMA-1 vaccinated C57BL/6 mice were re-challenged by RM-1 cells on day 7. Ten days after vaccination, CFSE-labeled OT-I CD8 + T-cells were injected into mice. On day 15 after vaccination, CFSE dilution of CD8 + T-cell in draining LNs was determined by using flow cytometry and ELISA. (b) Representative flow cytometry analyses of T-cell proliferation. (c) Quantitative data for T-cell proliferation (n = 4 per group). (d) ELISA analysis for FNγ production of CD8 + T-cell (n = 4 per group). Mice were vaccinated with DMSO- and Alternol-treated RM-1-Ova cells on day 0. Mice injected intraperitoneally 50 µg ovalbumin (257–264) peptide were used as a positive control. After 5 days of vaccination, LNs were extracted from mice and digested into single cells. CD8 + T cells in LNs were enriched and re-stimulated with ovalbumin (257–264) peptide (40 µg/ml) for 72 h, IFN-γ production in the culture medium was measured using an ELISA kit. (e) Schematic diagram of experiments for T cell block. On days −9, −8, 0, 7, mice were injected with anti-CD8+ antibody (for CD8 + T-cell depletion) at 10 mg/kg. IgG2b antibody was used as a control treatment. Mice were vaccinated with apoptotic tumor cell vaccination at day 0. Tumor volume (n = 10 per group) (f), tumor-free (n = 10, per group) (g) and survival (n = 10 per group) (h) were monitored as indication day.(i-l) T cell transfer was performed as indicated (i), tumor volume (n = 8 per group) (j), tumor-free (n = 10 per group) (k) and survival (n = 10 per group) (l) were monitored as indication day. Student's t-test was performed to determine the statistical significance of two groups (c, e). Statistical analysis of tumor growth, tumor-free progression, and animal overall survival was performed using two-way ANOVA analysis (g, k) and Log-rank (Mantel-Cox) test analysis, respectively (h, i, l, m). The asterisks indicate significant differences between the indicated groups (*** p < .001).
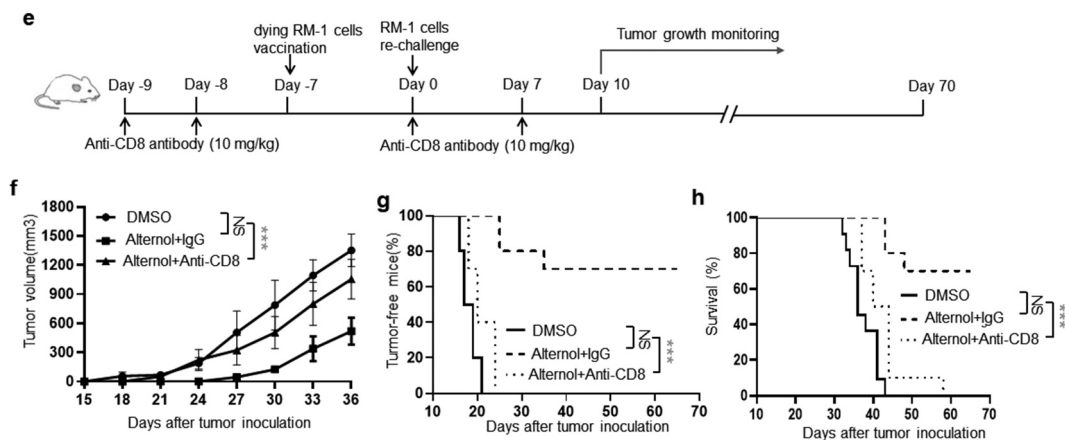
Figure 6. Continued.

inflammatory cytokines. Thus, our hypothesis in the present study was that Alternol triggered ICD *via* ROS generation-medicated inflammatory. NAC is a reduced glutathione (GSH) precursor, acting as a scavenger of ROS.[44] To validate this hypothesis, PC-3 cells were treated with DMSO, Alternol, NAC, or Alternol + NAC for 16 h. ROS inhibition blocked Alternol-induced upregulation of IL-8 (Figure 7c), IL-1A (Figure 7d), IL-6 (Figure 7e), and L-1β (Figure 7f) expression and that of eIF2α phosphorylation (Figure 7g, Supplemental Figure S9a-c), which is a biomarker of endoplasmic reticulum (ER) stress and ICD.[45] Our previous studies had shown that Alternol elevated ROS production by enhancing xanthine dehydrogenase (XDH) oxidative activity.[24] Febuxostat (FBX) is a selective inhibitor of XDH, which forms a stable complex with both the reduced and oxidized form of the enzyme, thereby inhibiting its function.[46] To validate the role of the XDH/ROS axis in Alternol-induced antitumor immune response, RM-1 cells were treated with DMSO, Alternol, Alternol+FBX or Alternol + NAC for 16 h and then C57BL/6 mice were vaccinated as showed in (Figure 7h). FBX and NAC treated significantly abolished Alternol-induced retarded tumor growth (Figure 7i), blocked Alternol-induced delayed tumor progression (Figure 7j), and eliminated Alternol-induced prolonged mice survival (Figure 7 k). These results
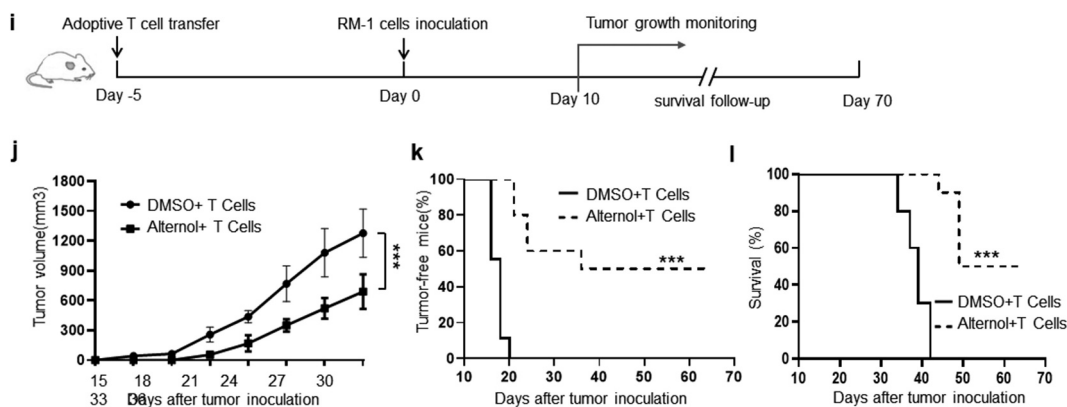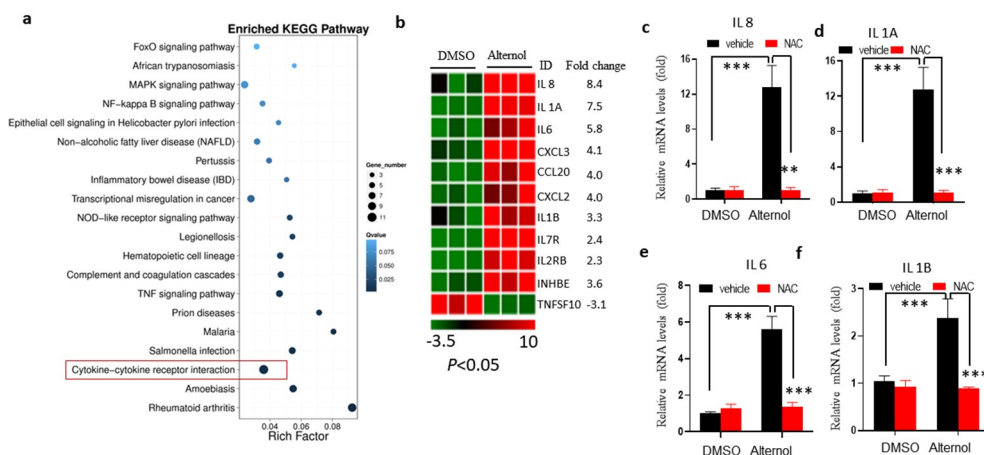
Figure 6. Continued.

Figure 7. ROS production is required for Alt-induced ICD. (a-b) PC-3 cells were treated with DMSO and Alternol (10 μM) for 16 h. Gene profiles were obtained by RNA sequencing. (a) KEGG analysis of upregulated genes in a gene set of PC-3 treated with Alternol. (b) Heat map of enriched genes in gene set of PC-3 treated with Alternol. (c-g) PC-3 cells were treated with DMSO, NAC (5 mM), Alternol (10 μM), Alternol (10 μM) + NAC (5 mM) for 16 h. (c-f) Real-time PCR analysis of upregulated inflammation cytokine genes in gene set of PC-3 with indicated treatment (n = 4). (g) eIF2α phosphorylation and eIF2α expression were determined by western blot. (h-k) Mice were vaccinated with RM-1 cells treated with DMSO, Alternol (10 μM), Alternol (10 μM)+NAC (5 mM), and Alternol (10 μM)+ FBX (20 μM). After one week of vaccination, mice were re-challenged with RM-1 cells (h). Tumor volume (n = 10 per group) (j) and survival (n = 10 per group) (k) were monitored as indication. Quantitative data are presented as means ± s.e.m. Statistical significance of multiple groups was measured by one-way ANOVA (b-f). Statistical analysis of tumor growth, tumor-free progression, and animal overall survival was performed using two-way ANOVA analysis (i) and Log-rank (Mantel-Cox) test analysis, respectively (j, k). The asterisks indicate significant differences between the indicated groups (*** $p < .001$).

indicate that Alternol-induced XDH/ROS pathway activation is necessary for the elicitation of Alternol-induced antitumor immune response.

Discussion

In the present study, Alternol was found to trigger ICD in prostate cancer cells, as evidenced by the increase in the release of DAMPs, pro-inflammatory cytokine expression, and anti-tumor immune response. Alternol treatment led to the activation of tumor-associated antigen uptake and cross-presentation of DCs, along with T-cell priming and infiltration in tumor-draining LNs, resulting in antitumor immune response. Moreover, blockade of ROS generation inhibited Alternol-driven ICD. This evidence suggests that Alternol triggers ICD in prostate cancer cells, which is mediated by ROS generation.

ICD induction induces ER stress and, consequently, the release of DAMPs.[39] The release of DAMPs enhances the rate of tumor cell phagocytosis by DCs, uptake and presentation of tumor-associated antigens to T-cells,[47] and inflammatory,[48] eventually resulting in immune activation against tumor growth. Several DAMPs have been identified and are involved in ICD, including (but not limited to) CALR, HMGB1, and ATP. In the present study, we found that Alternol triggered ICD, as evidenced by the increased the rate of HMGB1 and ATP release, and that of CALR translocation. Alternol enhanced the rates of cross-presentation and T-cell priming and infiltration, boosting the level of antitumor immunity in prostate cancer cells. Our previous studies have demonstrated that Alternol inhibits prostate cancer cell growth by disturbing the normal functioning of the Krebs cycle[34] and by increasing the rate of ROS production.[24] These findings suggest that Alternol may contribute to cytotoxicity, as suggested by
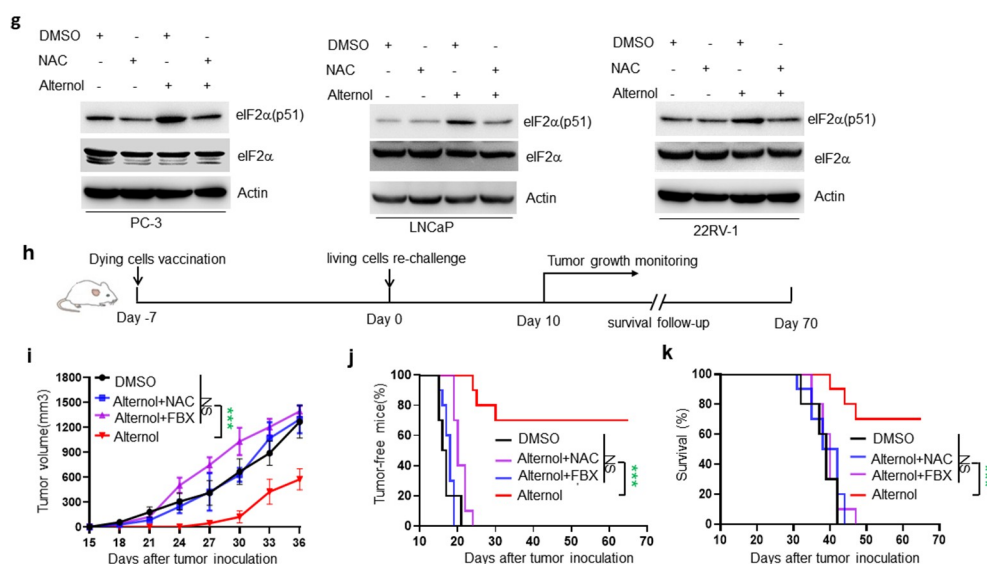
Figure 7. Continued.

previous studies, and may trigger anti-tumor immunity by inducing ICD.

The release of several pro-inflammatory cytokines is associated with cancer cells that undergo ICD, including IL-8,[49–52] IL-1α,[49,53] IL-1β,[49,50] IFN α/IFN β,[52] and IL-6.[50,52] Treatment with cetuximab, an ICD inducer,[30] promotes IL-1α secretion from head and neck squamous cell carcinoma cells. Increased levels of IL-1α expression in cancer cells enhance the rate of cetuximab-induced T-cell-dependent anti-tumor immune response.[53] Sukkurwala et al.[51] have reported that IL-8 is necessary for MTX-induced CALR exposure in HeLa cells. IL-8 inhibition reduces MTX-induced CALR exposure and subsequent ICD. In contrast, the addition of exogenous IL-8 increases the immunogenicity of dying cells in a CALR-dependent manner.[51] In the present study, we have shown that Alternol-treated prostate cancer cells exhibited elevated levels of pro-inflammatory cytokines (i.e., IL-1A, IL-1B, IL-8, and IL-6). Few studies have reported that pro-inflammatory cytokines may facilitate immunosuppression by activating T_{reg} cells and MDSCs.[54,55] However, upregulation of MDSCs was not associated with Alternol-induced elevation of pro-inflammatory cytokine levels in the present study. In contrast, mice vaccinated with Alternol-induced RM-1 cells that underwent cell death exhibited a lower percentage of T_{reg} cells, compared to control mice. This indicates that Alternol-induced inflammation may tip the balance toward antitumor immune activation responses rather than immunosuppression.

ROS are involved in various biological functions, including the generation of immune responses.[56,57] Accumulating evidence indicates that ROS are involved in ICD[12,57] and may mediate ICD by aggravating ER stress, or by activating the release of pro-inflammatory cytokines via the NLRP3 inflammasome, nuclear factor (NF)-$_K$B, and/or mitogen-activated protein kinase signaling pathways.[58] In the present study, ROS inhibition reduced Alternol-induced ER stress (measured with elevated eIF2a phosphorylation levels) and expression that of pro-inflammatory cytokine expression, eventually inhibiting Alternol-induced ICD. These findings suggest that ROS generation is involved in Alternol-induced ICD.

Although the adoption of immune checkpoint blockade (ICB)-based approaches has succeeded in preclinical studies and cancer clinical therapies for melanoma,[4–6] not all cancers are sensitive to ICB, specifically prostate cancer. Prostate cancer lacks a response to ICB and is considered an immunologically 'cold' tumor, which may be due to an insufficient number of somatic mutations or to an immunosuppressive microenvironment.[10,11,59] This study reveals that Alternol shifts the balance toward antitumor immune activation responses rather than immunosuppression, which may transform the 'cold' environment to a 'hot' one. Accumulating evidence indicates the clinical benefit of combining chemotherapies with immune checkpoint inhibitors (ICIs).[60] As such, the combination of Alternol and ICB may be exhibit enhanced antitumor activity for prostate cancer, compared with the use of Alternol or ICB alone. In future studies, we will investigate whether the combination of Alternol with ICB enhances immune response against prostate cancer.

Acknowledgments

Funding

ORCID

Changlin Li ⓘ http://orcid.org/0000-0001-5872-6443
Benyi Li ⓘ http://orcid.org/0000-0001-6242-5117

Data availability

RNA-seq data are available at http://www.ncbi.nlm.nih.gov/bioproject/705723 (BioProject ID: PRJNA705723). All data described in this study are available from the corresponding author upon request.

Authors' disclosures

All authors declare no conflicts of interest.

Author contributions

C.Li., Z. Q. and B. Li conceived and designed the experiments. Y. Zh. and S. Yuan developed methodology. Y. Zh, S. Yuan, G. Zh, and W. Wei acquired data. C. Li, and B. Li wrote, reviewed, and/or revised the manuscript.

References

1. Schostak M, Konig F, Bogemann M, Goebell P, Hammerer P, Machtens S, Schwentner C, Thomas C, von Amsberg G, von Rundstedt FC, et al., [Advanced Prostate Cancer Consensus Conference 2017: discussion of the recommendations for diagnosis and treatment of metastatic prostate cancer by a German panel of experts], Urologe A, 57 (2018) 813–820.

2. Kirby M, Hirst C, Crawford ED. Characterising the castration-resistant prostate cancer population: a systematic review. Int J Clin Pract. 2011;65(11):1180–1192. doi:10.1111/j.1742-1241.2011.02799.x.

3. Mansinho A, Macedo D, Fernandes I, Costa L. Castration-resistant prostate cancer: mechanisms, targets and treatment. Adv Exp Med Biol. 2018;1096:117–133.

4. Simpson TR, Li F, Montalvo-Ortiz W, Sepulveda MA, Bergerhoff K, Arce F, Roddie C, Henry JY, Yagita H, Wolchok JD, et al. Fc-dependent depletion of tumor-infiltrating regulatory T cells co-defines the efficacy of anti-CTLA-4 therapy against melanoma. J Exp Med. 2013;210(9):1695–1710. doi:10.1084/jem.20130579.

5. Chapuis AG, Lee SM, Thompson JA, Roberts IM, Margolin KA, Bhatia S, Sloan HL, Lai I, Wagener F, Shibuya K, et al. Combined IL-21-primed polyclonal CTL plus CTLA4 blockade controls refractory metastatic melanoma in a patient. J Exp Med. 2016;213:1133–1139. doi:10.1084/jem.20152021.

6. Schreibelt G, Bol KF, Westdorp H, Wimmers F, Aarntzen EH, Duiveman-de Boer T, van de Rakt MW, Scharenborg NM, De Boer AJ, Pots JM, et al. Effective clinical responses in metastatic melanoma patients after vaccination with primary myeloid dendritic cells. Clin Cancer Res. 2016;22:2155–2166. doi:10.1158/1078-0432.CCR-15-2205.

7. Ruiz-Cordero R, Devine WP. Targeted therapy and checkpoint immunotherapy in lung cancer. Surg Pathol Clin. 2020;13 (1):17–33. doi:10.1016/j.path.2019.11.002.

8. Emens LA. Breast cancer immunotherapy: facts and hopes. Clin Cancer Res. 2018;24(3):511–520. doi:10.1158/1078-0432.CCR-16-3001.

9. Maude SL, Laetsch TW, Buechner J, Rives S, Boyer M, Bittencourt H, Bader P, Verneris MR, Stefanski HE, Myers GD, et al. Tisagenlecleucel in children and young adults with B-cell lymphoblastic Leukemia. N Engl J Med. 2018;378(5):439–448. doi:10.1056/NEJMoa1709866.

10. Cha HR, Lee JH, Ponnazhagan S. Revisiting immunotherapy: a focus on prostate cancer. Cancer Res. 2020;80(8):1615–1623. doi:10.1158/0008-5472.CAN-19-2948.

11. Venturini NJ, Drake CG. Immunotherapy for prostate cancer. Cold Spring Harb Perspect Med. 2019;9(5):a030627. doi:10.1101/cshperspect.a030627.

12. Krysko DV, Garg AD, Kaczmarek A, Krysko O, Agostinis P, Vandenabeele P. Immunogenic cell death and DAMPs in cancer therapy. Nat Rev Cancer. 2012;12(12):860–875. doi:10.1038/nrc3380.

13. Kroemer G, Galluzzi L, Kepp O, Zitvogel L. Immunogenic cell death in cancer therapy. Annu Rev Immunol. 2013;31(1):51–72. doi:10.1146/annurev-immunol-032712-100008.

14. Zitvogel L, Apetoh L, Ghiringhelli F, Kroemer G. Immunological aspects of cancer chemotherapy. Nat Rev Immunol. 2008;8 (1):59–73. doi:10.1038/nri2216.

15. Fucikova J, Kralikova P, Fialova A, Brtnicky T, Rob L, Bartunkova J, Spisek R. Human tumor cells killed by anthracyclines induce a tumor-specific immune response. Cancer Res. 2011;71(14):4821–4833. doi:10.1158/0008-5472.CAN-11-0950.

16. Casares N, Pequignot MO, Tesniere A, Ghiringhelli F, Roux S, Chaput N, Schmitt E, Hamai A, Hervas-Stubbs S, Obeid M, et al. Caspase-dependent immunogenicity of doxorubicin-induced tumor cell death. J Exp Med. 2005;202(12):1691–1701. doi:10.1084/jem.20050915.

17. Suryadevara CM, Riccione KA, Sampson JH. Immunotherapy gone viral: bortezomib and oHSV enhance antitumor NK-cell activity. Clin Cancer Res. 2016;22(21):5164–5166. doi:10.1158/1078-0432.CCR-16-1666.

18. Tesniere A, Schlemmer F, Boige V, Kepp O, Martins I, Ghiringhelli F, Aymeric L, Michaud M, Apetoh L, Barault L, et al. Immunogenic death of colon cancer cells treated with oxaliplatin. Oncogene. 2010;29(4):482–491. doi:10.1038/onc.2009.356.

19. Liu P, Zhao L, Pol J, Levesque S, Petrazzuolo A, Pfirschke C, Engblom C, Rickelt S, Yamazaki T, Iribarren K, et al. Crizotinib-induced immunogenic cell death in non-small cell lung cancer. Nat Commun. 2019;10(1):1486. doi:10.1038/s41467-019-09415-3.

20. Humeau J, Sauvat A, Cerrato G, Xie W, Loos F, Iannantuoni F, Bezu L, Levesque S, Paillet J, Pol J, et al. Inhibition of transcription by dactinomycin reveals a new characteristic of immunogenic cell stress. EMBO Mol Med. 2020;12(5):e11622. doi:10.15252/emmm.201911622.

21. Obeid M, Tesniere A, Ghiringhelli F, Fimia GM, Apetoh L, Perfettini JL, Castedo M, Mignot G, Panaretakis T, Casares N, et al. Calreticulin exposure dictates the immunogenicity of cancer cell death. Nat Med. 2007;13(1):54–61. doi:10.1038/nm1523.

22. Alzeibak R, Mishchenko TA, Shilyagina NY, Balalaeva IV, Vedunova MV, Krysko DV. Targeting immunogenic cancer cell death by photodynamic therapy: past, present and future. J Immunother Cancer. 2021;9(1):e001926. doi:10.1136/jitc-2020-001926.

23. Fucikova J, Kepp O, Kasikova L, Petroni G, Yamazaki T, Liu P, Zhao L, Spisek R, Kroemer G, Galluzzi L. Detection of immunogenic cell death and its relevance for cancer therapy. Cell Death Dis. 2020;11(11):1013. doi:10.1038/s41419-020-03221-2.

24. Xu H, Li C, Mozzzicconacci O, Zhu R, Xu Y, Tang Y, Chen R, Huang Y, Holzbeierlein JM, Schoneich C, et al. Xanthine oxidase-mediated oxidative stress promotes cancer cell-specific apoptosis. Free Radic Biol Med. 2019;139:70–79. doi:10.1016/j.freeradbiomed.2019.05.019.

25. Tang Y, Chen R, Huang Y, Li G, Huang Y, Chen J, Duan L, Zhu BT, Thrasher JB, Zhang X, et al. Natural compound alternol induces oxidative stress-dependent apoptotic cell death preferentially in prostate cancer cells. Mol Cancer Ther. 2014;13(6):1526–1536. doi:10.1158/1535-7163.MCT-13-0981.

26. Liu ZZ, Zhu J, Sun B, Liu S, Geng S, Liu X, Li CL. Alternol inhibits proliferation and induces apoptosis in mouse lymphocyte leukemia (L1210) cells. Mol Cell Biochem. 2007;306(1–2):115–122. doi:10.1007/s11010-007-9560-0.

27. Zhu XL, Wang YL, Chen JP, Duan LL, Cong PF, Qu YC, Li-Ling J, Zhang MX. Alternol inhibits migration and invasion of human hepatocellular carcinoma cells by targeting epithelial-to-mesenchymal transition. Tumour Biol: J Int Soc Onco Dev Biol Med. 2014;35:1627–1635

28. Liu X, Wang J, Sun B, Zhang Y, Zhu J, Li C. Cell growth inhibition, G2M cell cycle arrest, and apoptosis induced by the novel compound Alternol in human gastric carcinoma cell line MGC803,

Invest. New Drugs. 2007;25(6):505–517. doi:10.1007/s10637-007-9057-4.

29. Li C, Xu H, Xiao L, Zhu H, Zhang G, Wei W, Li K, Cao X, Shen D, Holzbeierlein J, et al. CRMP4a suppresses cell motility by sequestering RhoA activity in prostate cancer cells. Cancer Biol Ther. 2018;19(12):1193–1203. doi:10.1080/15384047.2018.1491507.

30. Pozzi C, Cuomo A, Spadoni I, Magni E, Silvola A, Conte A, Sigismund S, Ravenda PS, Bonaldi T, Zampino MG, et al. The EGFR-specific antibody cetuximab combined with chemotherapy triggers immunogenic cell death. Nat Med. 2016;22(6):624–631. doi:10.1038/nm.4078.

31. Li C, Sun H, Wei W, Liu Q, Wang Y, Zhang Y, Lian F, Liu F, Li C, Ying K, et al. Mitoxantrone triggers immunogenic prostate cancer cell death via p53-dependent PERK expression. Cell Oncol (Dordr). 2020;43(6):1099–1116. doi:10.1007/s13402-020-00544-2.

32. Liu P, Zhao L, Kepp O, Kroemer G. Quantitation of calreticulin exposure associated with immunogenic cell death. Methods Enzymol. 2020;632:1–13.

33. Nam GH, Lee EJ, Kim YK, Hong Y, Choi Y, Ryu MJ, Woo J, Cho Y, Ahn DJ, Yang Y, et al. Combined Rho-kinase inhibition and immunogenic cell death triggers and propagates immunity against cancer. Nat Commun. 2018;9(1):2165. doi:10.1038/s41467-018-04607-9.

34. Li C, He C, Xu Y, Xu H, Tang Y, Chavan H, Duan S, Artigues A, Forrest ML, Krishnamurthy P, et al. Alternol eliminates excessive ATP production by disturbing Krebs cycle in prostate cancer. Prostate. 2019;79(6):628–639. doi:10.1002/pros.23767.

35. Oh DS, Lee HK. Autophagy protein ATG5 regulates CD36 expression and anti-tumor MHC class II antigen presentation in dendritic cells. Autophagy. 2019;15(12):2091–2106. doi:10.1080/15548627.2019.1596493.

36. Langmead B, Salzberg SL. Fast gapped-read alignment with Bowtie 2. Nat Methods. 2012;9(4):357–359. doi:10.1038/nmeth.1923.

37. Li B, Dewey CN. RSEM: accurate transcript quantification from RNA-Seq data with or without a reference genome. BMC Bioinform. 2011;12(1):323. doi:10.1186/1471-2105-12-323.

38. Love MI, Huber W, Anders S. Moderated estimation of fold change and dispersion for RNA-seq data with DESeq2. Genome Biol. 2014;15(12):550. doi:10.1186/s13059-014-0550-8.

39. Zhou J, Wang G, Chen Y, Wang H, Hua Y, Cai Z. Immunogenic cell death in cancer therapy: present and emerging inducers. J Cell Mol Med. 2019;23(8):4854–4865. doi:10.1111/jcmm.14356.

40. Takeuchi Y, Nishikawa H. Roles of regulatory T cells in cancer immunity. Int Immunol. 2016;28(8):401–409. doi:10.1093/intimm/dxw025.

41. Gabrilovich DI, Nagaraj S. Myeloid-derived suppressor cells as regulators of the immune system. Nat Rev Immunol. 2009;9(3):162–174. doi:10.1038/nri2506.

42. Groth C, Hu X, Weber R, Fleming V, Altevogt P, Utikal J, Umansky V. Immunosuppression mediated by myeloid-derived suppressor cells (MDSCs) during tumour progression. Br J Cancer. 2019;120(1):16–25. doi:10.1038/s41416-018-0333-1.

43. Galluzzi L, Buque A, Kepp O, Zitvogel L, Kroemer G. Immunogenic cell death in cancer and infectious disease. Nat Rev Immunol. 2017;17(2):97–111. doi:10.1038/nri.2016.107.

44. Aldini G, Altomare A, Baron G, Vistoli G, Carini M, Borsani L, Sergio F. N-Acetylcysteine as an antioxidant and disulphide breaking agent: the reasons why. Free Radic Res. 2018;52(7):751–762. doi:10.1080/10715762.2018.1468564.

45. Bezu, A. L, Sauvat J, Humeau LC, Gomes-da-Silva K, Iribarren S, Forveille P, Garcia L, Zhao P, Liu L, Zitvogel L, et al. eIF2alpha phosphorylation is pathognomonic for immunogenic cell death.

46. Gerriets V, Jialal I. Febuxostat. Treasure Island (FL): StatPearls; 2021.

47. Jeannin P, Jaillon S, Delneste Y. Pattern recognition receptors in the immune response against dying cells. Curr Opin Immunol. 2008;20(5):530–537. doi:10.1016/j.coi.2008.04.013.

48. Ghiringhelli F, Apetoh L, Tesniere A, Aymeric L, Ma Y, Ortiz C, Vermaelen K, Panaretakis T, Mignot G, Ullrich E, et al. Activation of the NLRP3 inflammasome in dendritic cells induces IL-1beta-dependent adaptive immunity against tumors. Nat Med. 2009;15 (10):1170–1178. doi:10.1038/nm.2028.

49. Pahk KJ, Shin CH, Bae IY, Yang Y, Kim SH, Pahk K, Kim H, Oh SJ. Boiling histotripsy-induced partial mechanical ablation modulates tumour microenvironment by promoting immunogenic cell death of cancers. Sci Rep. 2019;9(1):9050. doi:10.1038/s41598-019-45542-z.

50. Dudek-Peric AM, Ferreira GB, Muchowicz A, Wouters J, Prada N, Martin S, Kiviluoto S, Winiarska M, Boon L, Mathieu C, et al. Antitumor immunity triggered by melphalan is potentiated by melanoma cell surface-associated calreticulin. Cancer Res. 2015;75:1603–1614.

51. Sukkurwala AQ, Martins I, Wang Y, Schlemmer F, Ruckenstuhl C, Durchschlag M, Michaud M, Senovilla L, Sistigu A, Ma Y, et al. Immunogenic calreticulin exposure occurs through a phylogenetically conserved stress pathway involving the chemokine CXCL8. Cell Death Differ. 2014;21(1):59–68. doi:10.1038/cdd.2013.73.

52. Donnelly OG, Errington-Mais F, Steele L, Hadac E, Jennings V, Scott K, Peach H, Phillips RM, Bond J, Pandha H, et al. Measles virus causes immunogenic cell death in human melanoma. Gene Ther. 2013;20(1):7–15. doi:10.1038/gt.2011.205.

53. Espinosa-Cotton M, Rodman Iii SN, Ross KA, Jensen IJ, Sangodeyi-Miller K, McLaren AJ, Dahl RA, Gibson-Corley KN, Koch AT, Fu YX, et al. Interleukin-1 alpha increases anti-tumor efficacy of cetuximab in head and neck squamous cell carcinoma. J Immunother Cancer. 2019;7(1):79. doi:10.1186/s40425-019-0550-z.

54. Weber R, Groth C, Lasser S, Arkhypov I, Petrova V, Altevogt P, Utikal J, Umansky V. IL-6 as a major regulator of MDSC activity and possible target for cancer immunotherapy. Cell Immunol. 2021;359:104254. doi:10.1016/j.cellimm.2020.104254.

55. Dominguez C, McCampbell KK, David JM, Palena C. Neutralization of IL-8 decreases tumor PMN-MDSCs and reduces mesenchymalization of claudin-low triple-negative breast cancer. JCI Insight. 2017;2(21). doi:10.1172/jci.insight.94296.

56. Tavassolifar MJ, Vodjgani M, Salehi Z, Izad M. The influence of reactive oxygen species in the immune system and pathogenesis of multiple sclerosis. Autoimmune Dis. 2020;(2020):5793817.

57. Sun C, Wang H, Mao S, Liu J, Li S, Wang J. Reactive oxygen species involved in CT26 immunogenic cell death induced by Clostridium difficile toxin B. Immunol Lett. 2015;164(2):65–71. doi:10.1016/j.imlet.2015.02.007.

58. Waldmann TA. Cytokines in cancer immunotherapy. Cold Spring Harb Perspect Biol. 2018;10(12):a028472. doi:10.1101/cshperspect.a028472.

59. Tewari AK, Stockert JA, Yadav SS, Yadav KK, Khan I. Inflammation and Prostate Cancer. Adv Exp Med Biol. 2018;1095:41–65.

60. Galluzzi L, Humeau J, Buque A, Zitvogel L, Kroemer G. Immunostimulation with chemotherapy in the era of immune checkpoint inhibitors. Nat Rev Clin Oncol. 2020;17:725–741.

Cell Death Differ. 2018;25(8):1375–1393. doi:10.1038/s41418-017-0044-9.